Noise Design of Active Feedback Resonator BEF

Youhei Ishikawa, *Member, IEEE*, Sadao Yamashita, and Seiji Hidaka

***Abstract*—Active feedback resonator (AFR) filters can be used in design techniques for conventional passive microwave filters by introducing the noise temperature of a resonator. The noise figure (NF) of AFR filters can be analytically designed by using noise temperature. In this paper, three-pole AFR band elimination filter (BEF) is designed to evaluate the NF value. The measured results agree well with the theoretical values.**

I. Introduction

It is known that for small microwave resonators, the unloaded Q will generally deteriorate in proportion to the cube root of its volume [1]. The deterioration mainly originates from the Joule loss of a microwave electromagnetic field in a conductive shield. Several approaches using active elements or negative resistance have been introduced to recover a low-Q characteristic [2]. An active feedback resonator (AFR) [3], [4] has been proposed as a high-Q resonator that compensates for the energy loss of a passive resonator.

An AFR is a resonance circuit with high-Q characteristics. In the AFR, the resonator energy loss is compensated by an active feedback loop connected to the conventional microwave resonator. Because the AFR contains an active element, thermal noise should be taken into account when designing it. For this reason, the minimum noise design is an important problem for AFR design. We need a way to estimate the noise figure (NF) of an AFR filter easily when it is applied for receiver design because the NF is not negligible. However, no suitable circuit and noise design techniques have been known for the AFR filter design. Due to the complexity of the AFR circuit, complicated procedures of noise analysis are needed to evaluate the NF value.

According to circuit theory, an AFR can be expressed as a circuit equivalent to a passive resonator by introducing the noise temperature of the AFR [3]. It enables quantitative treatment of the thermal noise as well as simple analysis of AFR, so that AFR filter design can use design techniques for the conventional passive resonator filter. The NF value of the AFR filter can also be evaluated by measuring the noise temperatures of AFR's.

First, we describe the equivalent circuit and the noise temperature of AFR. Second, we discuss the NF analysis and a design example for the AFR BEF. And we make a total evaluation of an application of AFR BEF to a receiver design. Finally, we measure the NF value of a three-pole AFR BEF, and compared it with the theoretical value.

Manuscript received March 25, 1993; revised June 16, 1993.

The authors are with the Microwave Components Department I, Murata Manufacturing Company, Ltd., 26-10, 2-Chome, Tenjin, Nagaokakyo-shi, Kyoto 617, Japan.

IEEE Log Number 9213009.

II. Noise Temperature of AFR

As Fig. 1 shows, an AFR consists of an active feedback loop and a conventional passive resonator.

The low-noise amplifier shown in Fig. 1 will ideally amplify only the incident power with a gain of G. The parameters Q_0 and Q_{00} denote the unloaded Q with and without active feedback loop. The input and output ports of the active feedback loop are connected to the resonator with external Q's of Q_{e1} and Q_{e2}.

The resonance energy is positively fed back after being amplified by the low-noise amplifier. As a result, the AFR compensates for the power loss in the resonator, and enhances the equivalent unloaded Q in the resonator.

When the phase of the active feedback loop equals an integer times 2π, the resonance frequency of AFR is kept at the initial value and the unloaded Q is expressed by the following design formula [5]:

$$\frac{1}{Q_0} = \frac{1}{Q_{00}} + \frac{1}{Q_{e1}} + \frac{1}{Q_{e2}} - 2\sqrt{\frac{G}{Q_{e1}\,Q_{e2}}}. \tag{1}$$

Introducing the noise temperature T_n, the AFR in Fig. 1 can be expressed as the high-Q passive resonator with the temperature T_n shown in Fig. 2.

The symbols N_a and N_b in Fig. 1 denote the noise power generated at the output and input sides of the low-noise amplifier. Here, we will define the noise temperature T_a and T_b by the following equations:

$$\begin{aligned} N_a &\equiv GkT_aB \\ N_b &\equiv kT_bB \end{aligned} \tag{2}$$

where k is the Boltzmann constant and B the bandwidth. Using the noise temperatures defined by (2) and the white noise temperature T_0 (= 290 K), the noise temperature of AFR in Fig. 2 is defined by the following equation:

$$T_n \equiv \frac{Q_0}{Q_{00}}T_0 + \frac{Q_0}{Q_{e2}}GT_a + Q_0\left(\sqrt{\frac{1}{Q_{e1}}} - \sqrt{\frac{G}{Q_{e2}}}\right)^2 T_b. \tag{3}$$

If the parameters Q_0, Q_{00}, and G are specified in the electrical design of AFR, the optimum design minimizing the noise temperature [6] can be performed by the com-

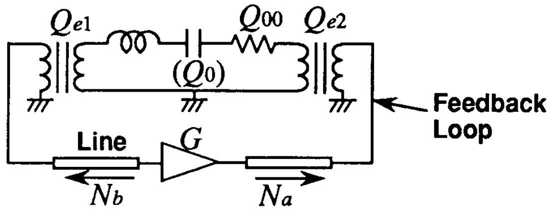

Fig. 1. Equivalent circuit of the AFR.

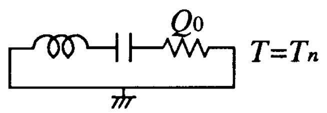

Fig. 2. Equivalent conversion of AFR circuit.

bination of Q_{e1} and Q_{e2} that satisfy the condition (1). This optimum design is an extreme value problem of (3) in which (1) is satisfied as a necessary condition, resulting in the following simple relation:

$$\frac{1}{Q_{e1}} = \frac{G}{Q_{e2}}. \tag{4}$$

The minimum noise temperature is expressed by

$$T_n|_{\min} = \frac{Q_0}{Q_{00}} T_0 + \frac{G}{G-1}\left(\frac{Q_0}{Q_{00}} - 1\right) T_a. \tag{5}$$

The first term on the right side of (5) represents the risen noise temperature of the interior resistance in proportion to the enhancement of unloaded Q, while the second term represents the minimum noise contribution from the amplifier.

III. Noise Design of AFR BEF

A. NF Analysis of AFR BEF

The following describes the NF analysis of AFR BEF. An equivalent circuit of AFR BEF is shown in Fig. 3.

In Fig. 3, f_{0l} denotes the resonance frequency, Q_{el} the external Q, Q_{0l} the unloaded Q, and T_{nl} ($l = 1, 2, \cdots, m$) the noise temperature of AFR. To clarify the noise sources of the resonators, Fig. 3 is converted as shown in Fig. 4.

In Fig. 4, we introduced m terminals connected to 50 Ω resistances with temperature of T_{nl} ($l = 1, 2, \cdots, m$). The noise power generated at these resistances are proportional to the temperatures and come out at input and output terminals of the BEF circuit. Denoting the transmission S parameter of BEF by S_{21} and the S parameters from the noise sources to the output terminal by $S_{2,l+2}$, the total noise power generated at the output terminal is expressed by the following equation:

$$N_{\text{out}} = |S_{21}|^2 N_{\text{in}} + \sum_{l=1}^{m} |S_{2,l+2}|^2 k T_{nl} B. \tag{6}$$

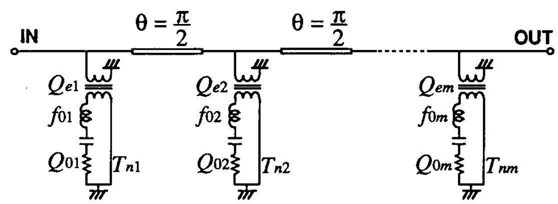

Fig. 3. Equivalent circuit of AFR BEF.

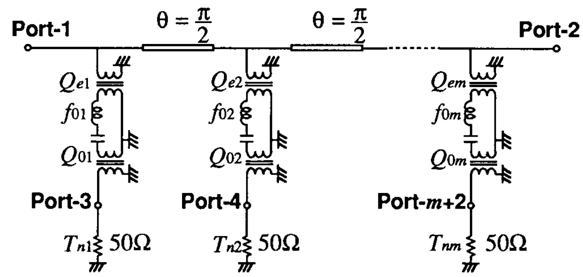

Fig. 4. Equivalent conversion of BEF circuit.

The signal output power S_{out} is expressed by the transmission S parameter S_{21} and signal input power S_{in}:

$$S_{\text{out}} = |S_{21}|^2 S_{\text{in}}. \tag{7}$$

Using (6), (7), and the definition of NF, the NF value of an AFR BEF is expressed as follows:

$$\begin{aligned} \text{NF} &\equiv 10 \log\left(\frac{S_{\text{in}}/N_{\text{in}}}{S_{\text{out}}/N_{\text{out}}}\right) \\ &= 10 \log\left(1 + \sum_{l=1}^{m} \frac{|S_{2,l+2}|^2 k T_{nl} B}{|S_{21}|^2 N_{\text{in}}}\right) \\ &= 10 \log\left(1 + \sum_{l=1}^{m} \frac{|S_{2,l+2}|^2}{|S_{21}|^2} \frac{T_{nl}}{T_0}\right). \end{aligned} \tag{8}$$

In the last arrangement of the equation, the incident noise power is assumed to equal the white noise power:

$$N_{\text{in}} = N_0 = k T_0 B. \tag{9}$$

As shown in the above procedures, the AFR BEF can readily be designed by expressing the AFR as a passive resonator with the temperature T_n. Minimizing the noise temperature of AFR enables minimum NF design for AFR BEF.

B. Design Example of AFR BEF

The following describes a design example of a three-pole AFR BEF that uses a Chebyshev filter [7]. The target characteristics of the three-pole AFR BEF are shown in Table I.

The equivalent circuit of a three-pole BEF is obtained by substituting 3 into m in Fig. 4. Table II shows example design parameters of a three-pole AFR BEF for the experiment.

TABLE I
TARGET CHARACTERISTICS OF THREE-POLE AFR BEF

Center frequency (f_0)	918.5 MHz
Attenuation at f_0 ± 0.12 MHz	15.0 dB min
Insertion Loss at f_0 ± 0.43 MHz	0.15 dB max
Noise Figure at f_0 ± 0.43 MHz	1.00 dB max

TABLE II
DESIGN PARAMETERS OF THREE-POLE AFR BEF

Pole No.	Resonance Frequency [MHz]	Unloaded Q	External Q
1	918.387	44 300	7390
2	918.494	47 100	4810
3	918.593	56 000	6600

The three-pole AFR BEF for the experiment is constructed of three sets of TM_{110} mode dielectric resonators, low-noise amplifiers, and connecting cables. The construction and the main construction elements of the three-pole AFR BEF are shown in Fig. 5 and Table III.

The calculation formula is obtained by substituting 3 into m in (8). The numerical values of S_{21}, S_{23}, S_{24}, and S_{25} required for the analysis are determined using a circuit simulator, as shown in Fig. 6.

The NF value of the three-pole AFR BEF can theoretically be calculated in accordance with (8) by using these S parameters and measured noise temperatures of AFR's. When the noise temperatures of all the AFR's are designed at 2700 K, for example, the NF of the three-pole AFR BEF is estimated by a circuit simulator as shown in Fig. 7. The IL of the three-pole AFR BEF is also shown in the same figure as a reference value. This simulation result satisfies the target characteristics shown in Table I.

C. Evaluation of AFR BEF as a Component of a Receiver

The following describes the evaluation of the AFR BEF as a component of a receiver. First, transmission and noise figure characteristics of the three-pole AFR BEF are evaluated compared with low-Q passive BEF. Second, total NF evaluation is made when the AFR BEF is applied to a receiver design. The low-Q passive BEF for comparison is an ideal Chebyshev BEF with unloaded Q of 7500 at each port. The external Q's have the same design values as the three-pole AFR BEF, as shown in Table II.

The transmission characteristics of AFR BEF and low-Q passive BEF are shown in Fig. 8.

The AFR BEF has an improved insertion loss in the passband when compared with the low-Q passive BEF. And more than 15 dB attenuation is obtained in the elimination band.

The NF characteristics of AFR BEF and low-Q passive BEF are calculated by using a circuit simulator, as shown in Fig. 9.

As Fig. 9 shows, the NF of the AFR BEF is almost the same as that of the low-Q passive BEF in the passband.

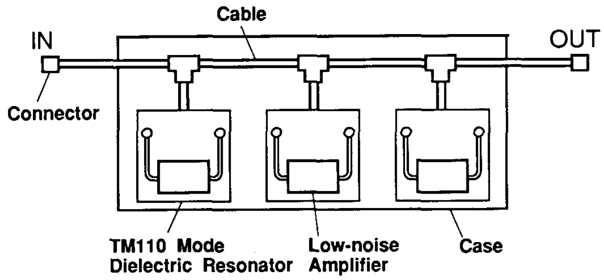

Fig. 5. Construction of the three-pole AFR BEF.

TABLE III
MAIN CONSTRUCTION ELEMENTS OF THE THREE-POLE AFR BEF

Resonator	
Mode	TM_{110}
Size	$53 \times 63 \times 67$ mm
ϵr	37
Connector	SMA
Cable	Semi-Rigid (UT085)
Amplifier	
Device	Bipolar Transistor (2SC4093)
Gain	12 dB
NF	2.6 dB (T_a = 240 K)

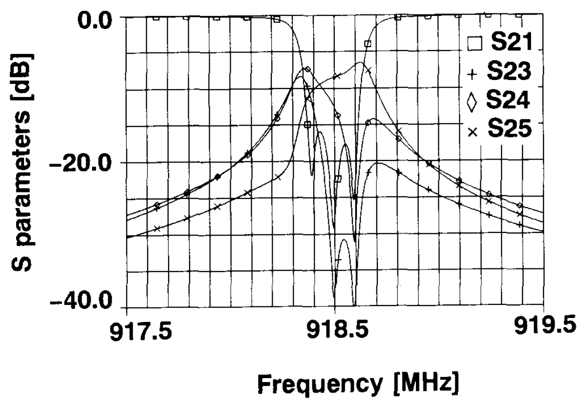

Fig. 6. S parameters of the three-pole BEF introduced three terminals.

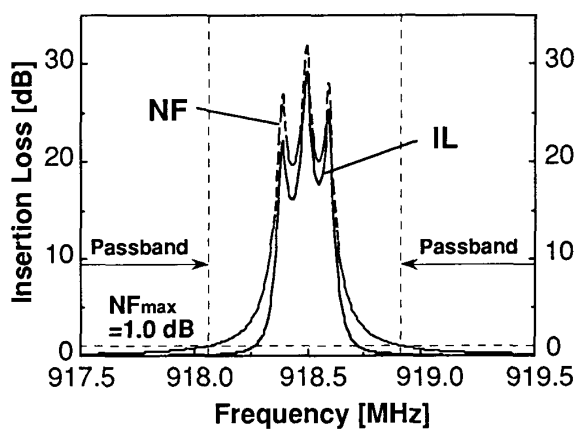

Fig. 7. NF estimation of the three-pole AFR BEF.

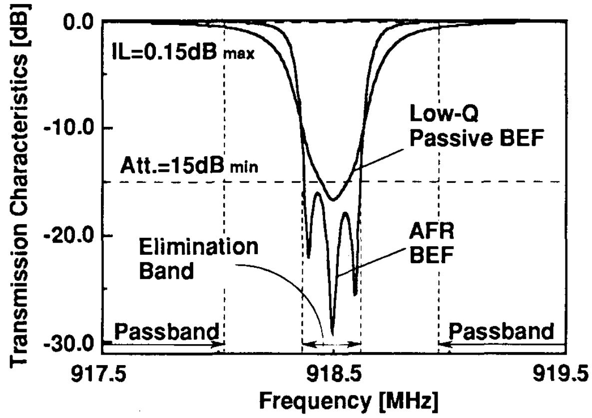

Fig. 8. Transmission characteristics of AFR BEF and passive BEF.

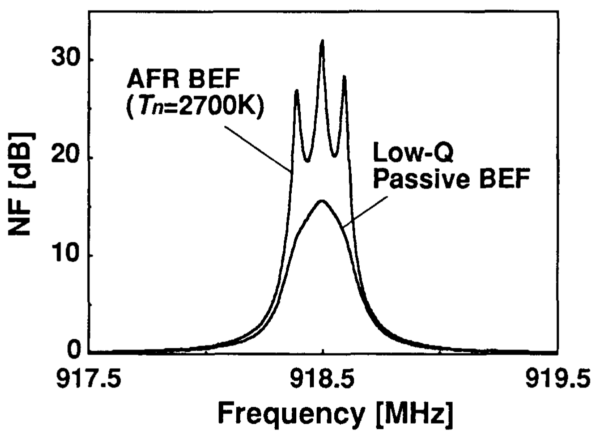

Fig. 9. NF characteristics of AFR BEF and passive BEF.

Although the NF of the AFR BEF is larger than that of low-Q passive BEF of the elimination band, it does not cause trouble because of the large attenuation level.

The following describes the total NF evaluation of a receiver composed of the three-pole AFR BEF and amplifying circuit shown in Fig. 10.

In the receiver in Fig. 10, an input signal is filtered by the BEF and amplified by the low-noise amplifier. The low-noise amplifier is assumed to be an ideal circuit with a gain of G', noise figure of NF$'$, and source impedance matched to the BEF circuit. When the receiver is constructed like this, the total NF of the receiver is calculated by using the following equation:

$$NF_{total} = 10 \log (10^{NF/10} + (10^{NF'/10} - 1) \times 10^{IL/10}). \tag{10}$$

As (10) shows, NF of BEF must be considered when it is not negligible compared with NF$'$ of the low-noise amplifier.

For a realistic numerical calculation, the low-noise amplifier of the receiver is assumed to have the gain (G') of 16 dB and noise figure (NF$'$) of 1.5 dB. The total NF of the receiver employing the three-pole AFR BEF is shown in Fig. 11. The NF of the conventional receiver employing low-Q passive BEF is also shown in the same figure for comparison.

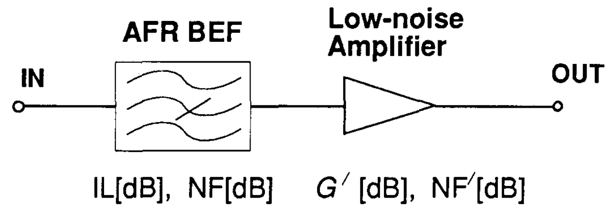

Fig. 10. Block diagram of receiver.

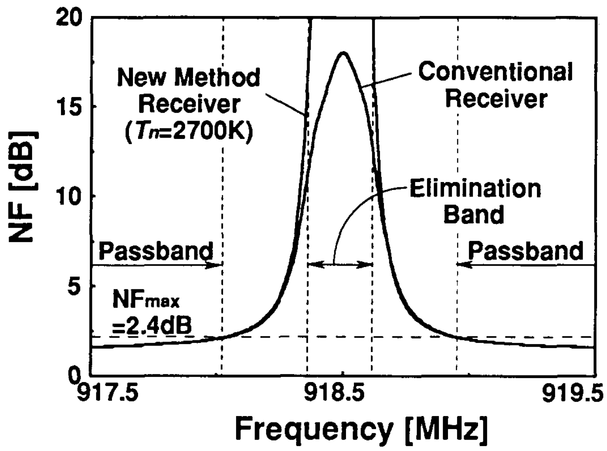

Fig. 11. Total NF of the receiver.

As Fig. 11 shows, the maximum NF of the receiver employing AFR BEF in the passband is about 2.4 dB, which is almost the same as that of the conventional receiver. But the attenuation of the receiver employing AFR BEF is improved in the elimination band.

IV. Experimental Results

This section compares the theoretical values with the experimental results of the three-pole AFR BEF that we designed. The minimum noise design of AFR was performed according to (4) and (5). The electrical length $\theta = \pi/2$ shown in Fig. 4 is determined around the center frequency of 918.5 MHz.

The theoretical calculation requires the noise temperatures of AFR's. The following describes the noise measurement procedure and results for a one-pole AFR BEF. Fig. 12 shows the noise temperature measurement system for a one-pole AFR BEF. A TM_{110} mode dielectric resonator with unloaded Q of about 7500 and low-noise amplifier with NF of 2.6 dB are used for this AFR [5]. As shown in Fig. 12, isolators are inserted at both sides of the low-noise amplifier to match the input and output loads. This structure realizes an ideal amplifying circuit

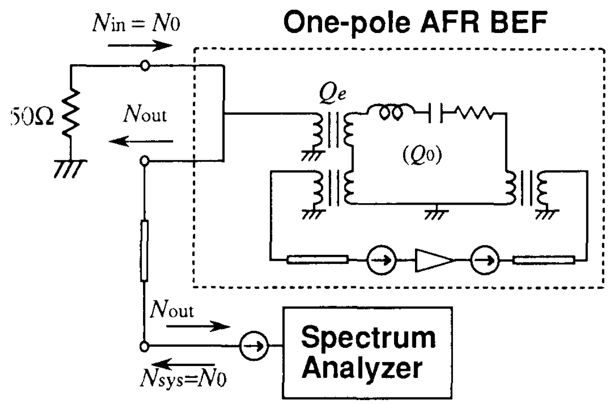

Fig. 12. Noise temperature measuring system for one-pole AFR BEF.

TABLE IV
MEASURED NOISE TEMPERATURE OF AFR

Pole No.	Noise Temperature [K]
1	2680
2	2740
3	2760

used in the analysis model which amplifies only the incident signal.

When N_{in} and N_{sys} are assumed to be the white noise power N_0, the formula for the noise temperature measurement is expressed by

$$T_n = T_0 + \frac{Q_e}{2Q_0}\left(1 + \frac{Q_0}{Q_e}\right)^2 \left(\frac{N'_{out}}{N'_0} \times 10^{NF_{sys}/10} - 1\right) T_0 \qquad (11)$$

where N'_{out}, N'_0 denote the noise power measured by a spectrum analyzer, and NF_{sys} the noise figure of the measuring instruments. Table IV shows the measured noise temperatures of AFR in accordance with (11).

The theoretical NF value of the three-pole AFR BEF can be calculated by substituting the noise temperatures shown in Table IV and S parameters shown in Fig. 6 into (8).

The following describes the NF measurement and its results of the three-pole AFR BEF. The diagram and external view of the NF measuring system are shown in Fig. 13.

The NF measurement formula for AFR BEF is expressed as the following equation:

$$NF = 10 \log \left(\frac{1}{|S_{21}|^2} \cdot \frac{N'_{out}}{N'_0} \times 10^{(NF_{sys}/10)} - \frac{|S_{22}|^2}{|S_{21}|^2} \right) \qquad (12)$$

where N'_{out} denotes the output noise power of three-pole AFR BEF measured by a spectrum analyzer.

The measured results of insertion loss and return loss of the three-pole AFR BEF are shown in Fig. 14.

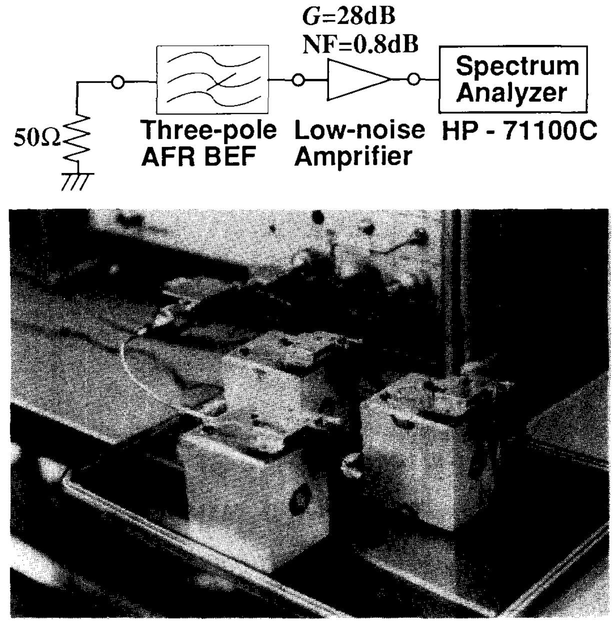

Fig. 13. NF measuring system for three-pole AFR BEF.

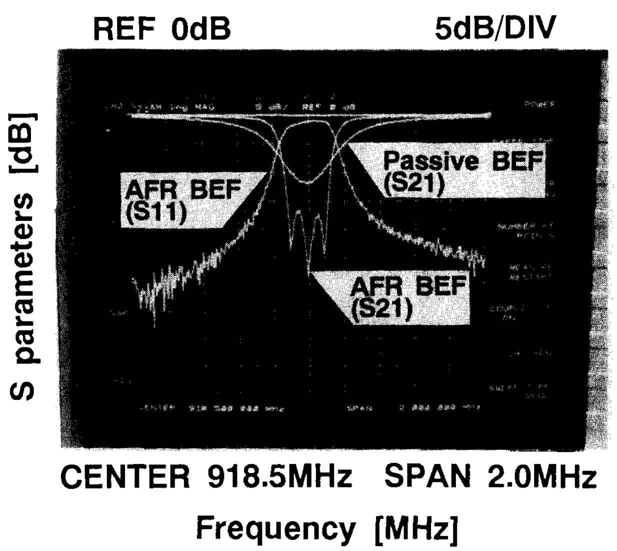

Fig. 14. S parameters of the three-pole AFR BEF.

The insertion loss of BEF without active feedback, that is, low-Q passive BEF with unloaded Q of about 3500 at each port, is also shown in Fig. 14. The magnitude of the S parameters S_{21} and S_{22} shown in (12) are measured by Fig. 14.

The noise output power of the three-pole AFR BEF is shown in Fig. 15.

The output noise power N'_{out} shown in (12) is measured by using the result of Fig. 15.

Fig. 16 shows the measured NF value obtained in accordance with NF measurement formula (12) and the the-

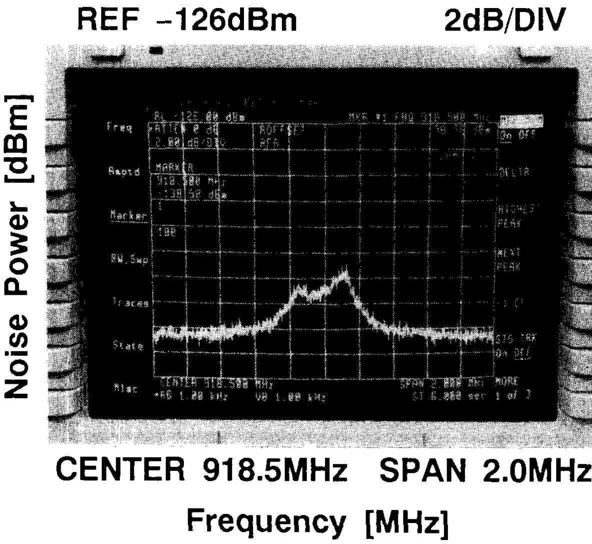

Fig. 15. Noise output of the three-pole AFR BEF.

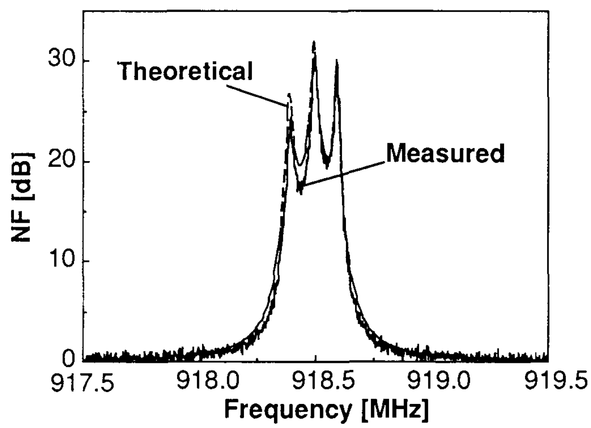

Fig. 16. Measured and theoretical NF values of the three-pole AFR BEF.

oretical NF value calculated in accordance with theoretical formula (8).

We find that the measured values agree with the theoretical value in the allowable error of noise amplitude.

V. Conclusions

In a filter design system which introduces noise temperature into the AFR, AFR BEF can be designed using techniques for the conventional passive BEF.

In this system, the passive BEF circuit used for electrical design is also useful for the noise analysis of the AFR BEF.

This analysis revealed that the NF value of the AFR BEF is calculated from the noise temperatures of AFR's. The minimum NF value is obtained by minimizing these noise temperatures.

A total NF evaluation is made when the AFR BEF is applied in a receiver design. The results showed that the NF of the receiver employing AFR BEF has almost the same value as that of a conventional receiver. But the attenuation in the elimination band of the receiver is improved.

The noise design of three-pole AFR BEF has been discussed in this study. It was found that the measured NF of the three-pole AFR BEF agrees well with the theoretical values deduced from the designed S parameters and the measured noise temperatures of AFR's.

References

[1] Y. Ishikawa, "Miniaturization technologies of dielectric resonator filter for mobile communication systems," in *MWE '92 Microwave Workshop Dig.*, 1992, pp. 351–356.

[2] T. Hirota and T. Itoh, "Recent progress in filters for mobile communications," in *URSI ISSSE Symp. Dig.*, Sept. 1992, pp. 856–858.

[3] H. Matsumura and Y. Konishi, "An active microwave filter with dielectric resonator," in *IEEE MTT-S Int. Microwave Symp. Dig.*, 1979, pp. 323–325.

[4] T. Nishikawa, H. Tanaka, J. Hattori, T. Kajikawa, and Y. Ishikawa, "400 MHz band active BEF using a bipolar transistor," in *Annu. Conf. IEICE, Dig. (Semiconductor Mater.)*, 1987, p. 219, 1987 (in Japanese).

[5] Y. Ishikawa, S. Yamashita, and S. Hidaka, "Noise temperature of active feedback feedback resonator (AFR)," *Tech. Rep. IEICE Japan*, MW92-102, pp. 39–46, 1993.

[6] Y. Ishikawa, J. Hattori, T. Sonoda, and S. Hidaka, "Sharp-cut dielectric duplexer for GSM-ETACS dual cellular systems using noise minimum AFR method," in *URSI ISSSE Symp. Dig.*, 1992, D7-3.

[7] G. L. Matthaei, L. Young, and E. M. T. Jones, *Microwave Filters, Impedance-Matching Networks, and Coupling Structures.* New York: McGraw-Hill, 1964, pp. 725–773.

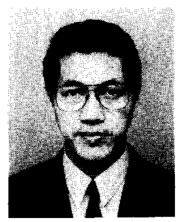

Youhei Ishikawa (M'77) was born in Kyoto, Japan, on October 4, 1946. He received the B.S. degree in physics from Kwansei Gakuin University, Hyogo, Japan, in 1970 and the M.S. degree in physics from the University of Nagoya, Aichi, Japan, in 1972.

He joined the Murata Manufacturing Company, Ltd., Kyoto, Japan in 1972. He has been engaged in the development of the microwave dielectric resonator and its application. He is currently a General Manager of the Microwave Components Development Department I, Technical Administration Division.

Mr. Ishikawa is a member of the Physical Society of Japan and the Institute of Electronics, Information, and Communication Engineers (IEICE) of Japan.

Sadao Yamashita was born in Kyoto Japan, on March 27, 1955.

He joined the Murata Manufacturing Company, Ltd., Kyoto, Japan in 1975. He is currently a Technical Staff member in the Microwave Components Development Department 1, Technical Administration Division.

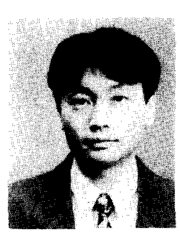

Seiji Hidaka was born in Hyogo, Japan, on May 9, 1965. He received the B.S. and M.S. degrees in physics from Kwansei Gakuin University, Hyogo, Japan, in 1988 and 1990, respectively.

He joined the Murata Manufacturing Company, Ltd., Kyoto, Japan, in 1990. He is currently a Technical Staff member in the Microwave Components Development Department 1, Technical Administration Division.

Mr. Hidaka is a member of the Institute of Electronics, Information, and Communication Engineers (IEICE) of Japan.